THE JOURNAL OF BIOLOGICAL CHEMISTRY VOL. 289, NO. 12, pp. 8668–8680, March 21, 2014

Lipopolysaccharide Engineering in *Neisseria meningitidis*

STRUCTURAL ANALYSIS OF DIFFERENT PENTAACYL LIPID A MUTANTS AND COMPARISON OF THEIR MODIFIED AGONIST PROPERTIES[*]

Received for publication, January 29, 2014 Published, JBC Papers in Press, February 3, 2014, DOI 10.1074/jbc.M114.554345

Elder Pupo[‡], **Hendrik-Jan Hamstra**[§], **Hugo Meiring**[‡], **and Peter van der Ley**[‡1]

From the [‡]*Institute for Translational Vaccinology and the* [§]*National Institute for Public Health and the Environment, 3721 MA Bilthoven, The Netherlands*

Background: LPS biosynthesis modification offers the potential to create detoxified variants with improved immunostimulatory properties.
Results: Pentaacyl LPS molecules from *pagL*$^+$ and *lpxL1*$^-$ meningococcal mutants were structurally characterized and found to activate human monocytic cells differentially.
Conclusion: PagL-deacylated meningococcal LPS has potential for human immunopotentiation.
Significance: These findings expand the knowledge on structure-function relationships of meningococcal LPS in relation to its immunomodulatory properties.

Engineering the lipopolysaccharide (LPS) biosynthetic pathway offers the potential to obtain modified derivatives with optimized adjuvant properties. *Neisseria meningitidis* strain H44/76 was modified by expression of the *pagL* gene encoding lipid A 3-*O*-deacylase from *Bordetella bronchiseptica* and by inactivation of the *lgtB* gene encoding the terminal oligosaccharide galactosyltransferase. Mass spectrometry analysis of purified mutant LPS was used for detailed compositional analysis of all present molecular species. This determined that the modified LPS was mainly pentaacylated, demonstrating high efficiency of conversion from the hexaacyl to the 3-*O*-deacylated form by heterologous lipid A 3-*O*-deacylase (PagL) expression. MS analyses also provided evidence for expression of only one major oligosaccharide glycoform, which lacked the terminal galactose residue as expected from inactivation of the *lgtB* gene. The immunomodulatory properties of PagL-deacylated LPS were compared with another pentaacyl form obtained from an *lpxL1*$^-$ mutant, which lacks the 2′ secondary acyl chain. Although both LPS mutants displayed impaired capacity to induce production of the pro-inflammatory cytokine IL-6 in the monocytic cell line Mono Mac 6, induction of the Toll-interleukin-1 receptor domain-containing adaptor-inducing interferon-β-dependent chemokine interferon-γ-induced protein 10 was largely retained only for the *lgtB*$^-$/*pagL*$^+$ mutant. Removal of remaining hexaacyl species exclusively present in *lgtB*$^-$/*pagL*$^+$ LPS demonstrated that these minor species potentiate but do not determine the activity of this LPS. These results are the first to indicate a qualitatively different response of human innate cells to pentaacyl *lpxL1*$^-$ and *pagL*$^+$ LPS and show the importance of detailed structure-function analysis when working with modified lipid A structures. The *pagL*$^+$ LPS has significant potential as immune modulator in humans.

Recognition of the lipid A moiety of lipopolysaccharide (LPS) through the TLR4·MD-2 receptor complex is one of the major activation events for innate immunity against Gram-negative bacteria. The signaling events following TLR4 activation involve two pathways, the MyD88-dependent pathway, which leads to the expression of pro-inflammatory gene products, and the TRIF-dependent pathway, leading to the expression of interferon-β and type I interferon-inducible genes (1). Many variations in the basic structure of lipid A exist, and they can influence the strength and nature of the evoked inflammatory response (2, 3). Such structure-function relationships are important determinants for the outcome of Gram-negative bacterial infections. Toll-like receptor activation is not only involved in the fast and relatively aspecific immediate response to infection, but also determines the strength and nature of the ensuing adaptive immune response. This is the basis of the strong adjuvant activity of LPS, and modification of lipid A structure allows the fine-tuning of this property to minimize excessive inflammatory responses while maintaining the desired immunostimulatory properties.

The human pathogen *Neisseria meningitidis* can cause life-threatening meningitis and sepsis, and many of the symptoms are ultimately caused by the LPS-triggered inflammatory response (4). The lipid A structure is a symmetric hexaacylated form that is an extremely potent TLR4·MD-2 activator. Interestingly, a significant proportion of meningococcal clinical isolates make a pentaacylated form instead, which lacks the 2′ secondary C12:0 acyl chain due to mutations in the *lpxL1* gene (5). The *lpxL1* LPS has a strongly reduced endotoxic activity, and disease caused by such mutants follows a milder, more protracted course.

* This work was supported by Marie Curie Intra-European Fellowship PIEF-GA-2009-252934 (to E. P.).
[1] To whom correspondence should be addressed: Institute for Translational Vaccinology, P. O. Box 450, 3720 AL Bilthoven, The Netherlands. Tel.: 31-30-274-2533; Fax: 31-30-274-2971; E-mail: peter.van.der.ley@intravacc.nl.

Outer membrane vesicles (OMVs)[2] have been investigated extensively as vaccines against meningococcal disease (6). They contain LPS with a hexaacylated lipid A, which functions as an effective adjuvant but also contributes to vaccine reactogenicity (7). Traditionally, LPS content is reduced by a detergent extraction step, mostly with deoxycholate. Although effective in reducing the endotoxic activity, this also has serious drawbacks, especially the loss of lipoproteins that can be important protective antigens. The use of attenuated LPS forms, such as *lpxL1*, provides an attractive alternative, as there is no longer a need to extract it for reducing endotoxic activity (8). Native OMVs containing *lpxL1* LPS display a proinflammatory activity similar to deoxycholate-extracted OMVs with wild-type LPS, and they have shown no adverse effects in the first clinical trials.

Although *lpxL1* LPS has a strongly reduced endotoxic activity due to the loss of the secondary C12:0 acyl chain at the 2′-position, it may not be optimal in terms of adjuvant activity. Minor variations in lipid A structure can affect these properties, and in this study we have investigated an alternative form of pentaacylated meningococcal LPS created by enzymatic modification. The PagL outer membrane-located enzyme specifically deacylates lipid A at the 3-position (9). It is found in a variety of Gram-negative bacteria but not in *N. meningitidis*. We have previously studied its effects in the *Bordetella*, where it is found in *Bordetella bronchiseptica* but not in *Bordetella pertussis* where only a pseudogene is present (10, 11). We now report its activity in *N. meningitidis* and provide a detailed structural analysis of the PagL-modified LPS. In addition, we demonstrate that the PagL-deacylated LPS displays different pro-inflammatory properties compared with *lpxL1* LPS, and it may have promise for use as a novel adjuvant.

EXPERIMENTAL PROCEDURES

Bacterial Strains and Plasmids—*N. meningitidis* strains were grown on GC medium base (Difco) supplemented with IsoVitaleX, and the required antibiotics, in a humid atmosphere containing 5% CO_2 at 37 °C. For isolation of LPS, bacteria grown in a chemically defined liquid medium were used (12). The *galE*$^-$ *lpxL1*$^-$ mutant derivative of *N. meningitidis* strain H44/76 was obtained by transformation with plasmid pMF121 and pBSNK6 to erythromycin and kanamycin resistance, respectively, resulting in deletion of the capsular biosynthesis locus, including the *galE* gene, and insertional inactivation of *lpxl1* (13, 14). For expression of *B. bronchiseptica pagL*, a derivative of plasmid pEN11 carrying it behind a *lac* promotor (11) was introduced into an H44/76 strain with insertionally inactivated *siaD* and *lgtB* genes. This strain was grown in medium with or without 1 mM IPTG, to compare the effect of *pagL* induction on lipid A deacylation. Bacteria with and without *pagL* induction are denoted as *lgtB*$^-$ *pagL*$^+$ and *lgtB*$^-$ only, respectively. Primers used for PCR verification of mutations were as follows: siaC F, 5′-CGCAAAGGTGCTCAAATC-3′; siaD R, 5′-AGGCCAGGCCTATAATTC-3′, pagL F, 5′-ATGCAATTTCTCAAG-3′, and pagL R, 5′-TCAGAACTGGTACGT-3′; lgtB F, 5′-TTGGTCAAGGCGCGGATC-3′, and lgtB R, 5′-AGGGCGCACATTGCCGATAC-3′; lpxL1 F, 5′-GACTCGAAACGCCTGATATG-3′, and lpxL1 R, 5′-GTTTGCTTGCCTACCTTCTG-3′.

Lipopolysaccharides—The LPS from the *lgtB*$^-$, *lgtB*$^-$ *pagL*$^+$, and *galE*$^-$ *lpxL1*$^-$ mutants of *N. meningitidis* were obtained by the hot phenol/water method (15) and further purified using diafiltration and differential centrifugation. The extracted LPS was diafiltrated against 10 mM $MgCl_2$ by cross-flow filtration through a 10-kDa filter to remove traces of phenol and further purified from nucleic acid and protein contamination by sequential treatment with 100 units/ml of Benzonase® endonuclease (VWR International BV, Amsterdam, The Netherlands) at 35 °C for 6 h and 50 μg/ml of proteinase K (VWR International BV, Amsterdam, The Netherlands) at 35 °C for 12 h. Then the LPS was recovered by centrifugation at 16,000 × *g* for 15 min at 20–25 °C and brought in suspension with an aqueous solution of 100 mM EDTA. Subsequently, the LPS was diafiltrated against 1 mM Tris-HCl, pH 7.5, by cross-flow filtration through a 10-kDa filter, heated at 70 °C for 30 min, cooled down to 20–25 °C, and finally sterile-filtered through a 0.2-μm filter. Residual protein content was assayed by the method of Peterson (16) and nucleic acid contamination was determined by ethidium bromide fluorescence (17). Both were below the detection limit. LPS concentration was determined by the KDO assay (18).

Mass Spectrometry—Negative ion electrospray ionization-Fourier transform-mass spectrometry (ESI-FT-MS) was performed on an LTQ Orbitrap XL instrument (Thermo Scientific). LPS samples were dissolved in a mixture of 2-propanol, water, and triethylamine 50:50:0.001 (v/v/v), pH 8.5, and infused into the FT-MS by static nano-ESI (19, 20). The spray voltage was set to −2.3 kV and the capillary temperature to 200 °C. Under these ionization conditions, no appreciable fragmentation of LPS was produced. Y- and B-type fragment ions, corresponding to the lipid A and oligosaccharide moieties of LPS, respectively, were generated by in-source collision-induced dissociation (SID) at a potential difference of 100 V (19). Fragment ions were annotated according to the nomenclature of Domon and Costello (21). The mass scale was calibrated internally with taurocholic acid following standard procedures provided by the manufacturer. Mass-to-charge ratios given refer to mono-isotopic molecular masses. The Glyco-Peakfinder online software was used to calculate the mass-to-charge ratio and deviation of theoretical LPS composition proposals (22). LPS composition proposals were based on the general chemical structure of the L3-immunotype LPS from *N. meningitidis* reported previously (Fig. 1) (23, 24).

Cytokine Induction in Mono Mac 6 Cells—Human monocytic MM6 cells (25) were seeded in 96-well microtiter plates (1.5×10^5 cells per well) in 100 μl of Iscove's modified Dulbecco's medium (IMDM) (Invitrogen) supplemented with 100 units/ml penicillin, 100 μg/ml streptomycin, 292 μg/ml L-glutamine

[2] The abbreviations used are: OMV, outer membrane vesicle; PagL, lipid A 3-*O*-deacylase; MyD88, myeloid differentiation primary response gene 88; TRIF, Toll-interleukin-1 receptor domain-containing adaptor inducing interferon-β; ESI-FT-MS, electrospray ionization-Fourier transform mass spectrometry; SID, in-source collision-induced dissociation; MM6, mono mac 6; IMDM, Iscove's modified Dulbecco's medium; IP-10, interferon-γ-induced protein 10; DC, dendritic cell; DC-SIGN, dendritic cell-specific intercellular adhesion molecule 3-grabbing nonintegrin; PEA, phosphoethanolamine; C12:0(3-OH), 3-hydroxy-dodecanoic acid; C12:0, dodecanoic acid; TEA, triethylamine; F, forward; R, reverse; IPTG, isopropyl 1-thio-β-D-galactopyranoside.

(Invitrogen), and 10% fetal calf serum (Invitrogen). Subsequently, cells were stimulated with 100 μl of serial dilutions of LPS in supplemented IMDM for 16–18 h at 37 °C in a humid atmosphere containing 5% CO_2. Cytokine concentrations in the supernatants were determined by enzyme-linked immunosorbent assay (ELISA) using a PeliPair™ reagent set (Sanquin) (for IL-6 and IL-10) and a DuoSet® ELISA development kit (R&D Systems) (for IP-10); following the manufacturer's instructions.

Mild Alkaline Hydrolysis of LPS in 5% Triethylamine—A very mild alkaline hydrolysis of the LPS in the presence of 5% triethylamine was performed with the aim of removing minor hexaacylated LPS species, containing 3-*O*-linked fatty acids, in the mostly pentaacylated and 3-*O*-deacylated LPS from the *lgtB*$^-$ *pagL*$^+$ mutant of *N. meningitidis*. To this end, the lipopolysaccharides (520 μg) were suspended in 2 ml of 5% triethylamine and incubated at 45 °C for 3 h under agitation. Then, the reaction was stopped by neutralizing the pH of the mixture with 10% acetic acid. As negative control for the 3-*O*-deacylation reaction, 520 μg of LPS from the *lgtB*$^-$ *pagL*$^+$ mutant were suspended in 2 ml of 5% triethylamine at room temperature, and the mixture was immediately neutralized with 10% acetic acid and then kept for 3 h at room temperature under agitation. As a positive control for the 3-*O*-deacylation reaction, 200 μg of LPS from the hexaacylated *lgtB*$^-$ LPS mutant were suspended in 2 ml of 5% triethylamine and incubated at 45 °C for 4 h under agitation. Then, the reaction was stopped by neutralizing the pH of the mixture with 10% acetic acid. Subsequently, LPS mixtures were freeze-dried overnight and desalted by three consecutive precipitations of LPS with 90% ethanol. Finally, the extent of LPS 3-*O*-deacylation was monitored by ESI-FT-MS analysis as described above.

Competitive Inhibition of IL-6 Inducing Activity of Hexaacylated LPS from lgtB$^-$ *Mutant in MM6 Cells by Pentaacylated LPS from lgtB*$^-$ *pagL*$^+$ *and galE*$^-$ *lpxL1*$^-$ *Mutants*—A total of 2.5 ng/ml of LPS from the *lgtB*$^-$ mutant was mixed with from 0.24 to 15.6 ng/ml of LPS from the *lgtB*$^-$ *pagL*$^+$ or *galE*$^-$ *lpxL1*$^-$ mutants in IMDM supplemented as described above. Then, MM6 cells were stimulated with LPS mixtures in supplemented IMDM for 16–18 h at 37 °C in a humid atmosphere containing 5% CO_2. IL-6 concentrations in the supernatants were determined by ELISA using a PeliPair™ reagent set (Sanquin) according to the manufacturer's instructions. Statistically significant differences ($p < 0.05$) in the level of IL-6 produced by MM6 cells were determined by the Mann-Whitney test by using GraphPad Prism 6.0 statistical software (GraphPad Software, Inc.).

RESULTS

Construction of an N. meningitidis Strain with Inducible Expression of B. bronchiseptica PagL LPS Deacylase—For the conditional deacylation of LPS, a derivative of meningococcal strain H44/76 was constructed in the following way. First, the *siaD* gene was inactivated by insertion of an erythromycin-resistance cassette, leading to the loss of the serogroup B polysialyltransferase and thereby to capsular polysaccharide deficiency. Second, the *lgtB* gene was inactivated by insertion of a kanamycin-resistance cassette, leading to loss of the terminal Gal residue of the LPS oligosaccharide and exposing a

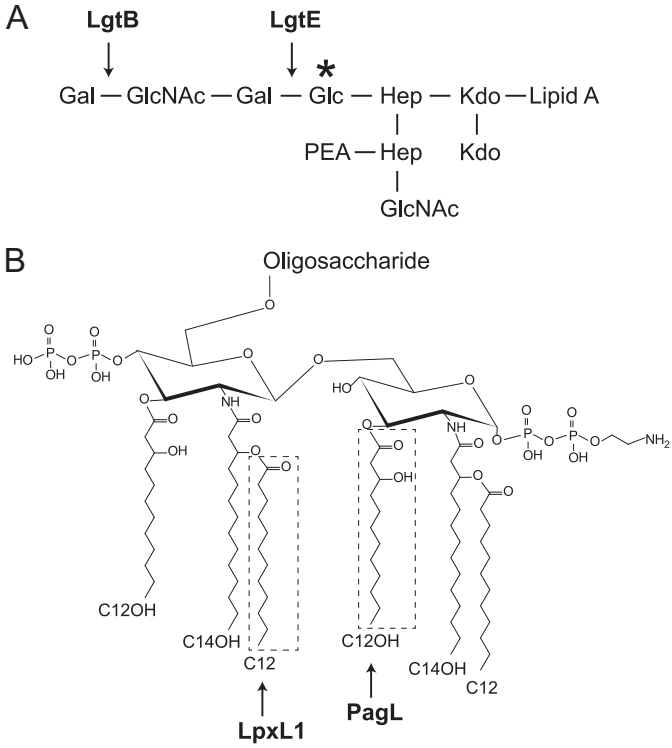

FIGURE 1. **Schematic representation of the chemical structure of the lipopolysaccharide of wild-type *N. meningitidis* strain H44/76 (L3-immunotype) (23, 24).** The sites of action of the lipopolysaccharide glycosyltransferases B and E in LPS oligosaccharide (*A*) and those of the lipid A fatty acyltransferase (*LpxL1*) and 3-*O*-deacylase PagL (*B*) are indicated. In *galE* mutants, the oligosaccharide chain is expected to terminate at the glucose residue shown by an *asterisk*. Abbreviations used are as follows: *Kdo,* 3-deoxy-D-*manno*-oct-2-ulosonic acid; *Hep,* heptose.

DC-SIGN-binding site (26). Third, a plasmid pEN11 derivative carrying the *B. bronchiseptica pagL* gene behind a *lac* promoter was introduced by selection for chloramphenicol-resistant transformants. The presence of inactivated chromosomal *siaD* and *lgtB* genes and the plasmid-encoded *pagL* gene was verified by PCR. The strain was grown in medium with or without 1 mM IPTG to compare the effect of *pagL* induction on lipid A deacylation. MS analysis of lipid A obtained after mild acid hydrolysis of purified LPS was performed to determine the degree of deacylation at the 3-position (data not shown). Without *pagL* induction, the lipid A was mostly in the hexaacyl form, whereas with induction only the pentaacyl form lacking a C12:0(3-OH) fatty acyl chain was observed, showing that the *B. bronchiseptica* PagL enzyme was active in *N. meningitidis* and its expression controlled by induction with IPTG. H44/76 *siaD lgtB* bacteria carrying the pEN11-*pagL* plasmid with and without *pagL* induction are denoted as *lgtB*$^-$*pagL*$^+$ and *lgtB*$^-$ only, respectively.

Mass Spectrometric Characterization of Complete LPS—The structural heterogeneity of LPS from the mutant strains of *N. meningitidis* was characterized by ESI-FT-MS. The triply charged $[M - 3H]^{3-}$ molecular ion regions of the mass spectra of intact LPS are presented in Fig. 2. The mass spectra of the LPS from the *lgtB*$^-$ mutant grown in the absence of IPTG (Fig. 2*A*) was dominated by a signal of a $[M - 3H]^{3-}$ molecular ion (*m/z* 1196.867), which is consistent with the LPS species being comprised of an L3-immunotype oligosaccharide structure (Fig. 1*A*), lacking the terminal galactose (Gal) residue, as

TABLE 1

Proposed compositions for the triply charged $[M - 3H]^{3-}$ molecular ions observed in ESI-FT-MS of intact LPS from *lgtB*$^-$, *lgtB*$^-$ *pagL*$^+$, and *galE*$^-$ *lpxL1*$^-$ mutants of *N. meningitidis* (Fig. 2)

Abbreviations used are as follows: Kdo, 3-deoxy-D-*manno*-oct-2-ulosonic acid; Hep, L-*glycero*-D-*manno*-heptose; Hex, hexose; HexNAc, *N*-acetylhexosamine; Gly, glycine; P, phosphate; $C_{12}OH$, 3-hydroxy-dodecanoic acid; $C_{14}OH$, 3-hydroxy-tetradecanoic acid; C_{12}, dodecanoic acid.

LPS	Ion type	Measured *m/z*	Proposed LPS composition		Calculated *m/z*	Deviation (ppm)
			Oligosaccharide	Lipid A		
lgtB$^-$	$[M-3H]^{3-}$	1089.810	Hex**2**•HexNAc**2**• Hep**2**•PEA**1**•Kdo**2**	HexN**2**•P**3**•C_{12}OH**1**•C_{14}OH**2**•C_{12}**2**	1089.808	2.3
	$[M-3H]^{3-}$	1129.207	Hex**2**•HexNAc**2**• Hep**2**•PEA**1**•Kdo**2**	HexN**2**•P**2**•C_{12}OH**2**•C_{14}OH**2**•C_{12}**2**	1129.206	0.8
	$[M-3H]^{3-}$	1130.813	Hex**2**•HexNAc**2**• Hep**2**•PEA**1**•Kdo**2**	HexN**2**•P**3**•PEA**1**•C_{12}OH**1**•C_{14}OH**2**•C_{12}**2**	1130.810	2.3
	$[M-3H]^{3-}$	1136.146	Hex**2**•HexNAc**2**• Hep**2**•PEA**1**•Kdo**2**	HexN**2**•P**3**•PEA**1**•C_{12}OH**2**•C_{14}OH**2**•C_{12}**1**	1136.142	3.5
	$[M-3H]^{3-}$	1146.520	Hex**2**•HexNAc**2**• Hep**2**•PEA**1**•Kdo**2**	HexN**2**•P**3**•C_{12}OH**2**•C_{14}OH**2**•C_{12}**2** -C_2H_4	1146.518	1.9
	$[M-3H]^{3-}$	1155.863	Hex**2**•HexNAc**2**• Hep**2**•PEA**1**•Kdo**2**	HexN**2**•P**3**•C_{12}OH**2**•C_{14}OH**2**•C_{12}**2**	1155.862	1.3
	$[M-3H]^{3-}$	1170.211	Hex**2**•HexNAc**2**• Hep**2**•PEA**1**•Kdo**2**	HexN**2**•P**2**•PEA**1**•C_{12}OH**2**•C_{14}OH**2**•C_{12}**2**	1170.209	1.8
	$[M-3H]^{3-}$	1187.523	Hex**2**•HexNAc**2**• Hep**2**•PEA**1**•Kdo**2**	HexN**2**•P**3**•PEA**1**•C_{12}OH**2**•C_{14}OH**2**•C_{12}**2** -C_2H_4	1187.521	2.0
	$[M-3H]^{3-}$	1196.867	Hex**2**•HexNAc**2**• Hep**2**•PEA**1**•Kdo**2**	HexN**2**•P**3**•PEA**1**•C_{12}OH**2**•C_{14}OH**2**•C_{12}**2**	1196.864	2.2
lgtB$^-$ *pagL*$^+$	$[M-3H]^{3-}$	1130.811	Hex**2**•HexNAc**2**• Hep**2**•PEA**1**•Kdo**2**	HexN**2**•P**3**•PEA**1**•C_{12}OH**1**•C_{14}OH**2**•C_{12}**2**	1130.810	0.5
	$[M-3H]^{3-}$	1171.813	Hex**2**•HexNAc**2**• Hep**2**•PEA**1**•Kdo**2**	HexN**2**•P**3**•PEA**2**•C_{12}OH**1**•C_{14}OH**2**•C_{12}**2**	1171.813	0.2
	$[M-3H]^{3-}$	1190.821	Hex**2**•HexNAc**2**• Hep**2**•Gly**1**•PEA**1**•Kdo**2**	HexN**2**•P**3**•PEA**2**•C_{12}OH**1**•C_{14}OH**2**•C_{12}**2**	1190.820	0.5
	$[M-3H]^{3-}$	1196.863	Hex**2**•HexNAc**2**• Hep**2**•PEA**1**•Kdo**2**	HexN**2**•P**3**•PEA**1**•C_{12}OH**2**•C_{14}OH**2**•C_{12}**2**	1196.864	1.2
	$[M-3H]^{3-}$	1237.865	Hex**2**•HexNAc**2**• Hep**2**•PEA**1**•Kdo**2**	HexN**2**•P**3**•PEA**2**•C_{12}OH**2**•C_{14}OH**2**•C_{12}**2**	1237.867	1.8
galE$^-$ *lpxL1*$^-$	$[M-3H]^{3-}$	1014.424	Hex**1**•HexNAc**1**• Hep**2**•PEA**1**•Kdo**2**	HexN**2**•P**3**•PEA**1**•C_{12}OH**2**•C_{14}OH**2**•C_{12}**1**	1014.431	7.3
	$[M-3H]^{3-}$	1055.426	Hex**1**•HexNAc**1**• Hep**2**•PEA**1**•Kdo**2**	HexN**2**•P**3**•PEA**2**•C_{12}OH**2**•C_{14}OH**2**•C_{12}**1**	1055.434	7.8
	$[M-3H]^{3-}$	1068.442	Hex**2**•HexNAc**1**• Hep**2**•PEA**1**•Kdo**2**	HexN**2**•P**3**•PEA**1**•C_{12}OH**2**•C_{14}OH**2**•C_{12}**1**	1068.449	6.5
	$[M-3H]^{3-}$	1109.442	Hex**2**•HexNAc**1**• Hep**2**•PEA**1**•Kdo**2**	HexN**2**•P**3**•PEA**2**•C_{12}OH**2**•C_{14}OH**2**•C_{12}**1**	1109.452	8.8

expected for the inactivation of the *lgtB* gene, and a wild-type hexaacyl lipid A structure (Fig. 1*B*), carrying three phosphates and a phosphoethanolamine (PEA) (see Table 1 for LPS composition proposals). Also, two $[M - 3H]^{3-}$ molecular ions of relatively lower abundance (*m/z* 1170.211 and 1155.863) (Fig. 2*A*) were detected, which account for LPS containing a phosphate and a PEA residue less than the main LPS species, respectively. Other minor $[M - 3H]^{3-}$ molecular ions were present, which can be attributed to LPS species which, as compared with the main LPS structure, have one or two fatty acyl chains one or two carbons shorter (*m/z* 1187.523), contain one less dodecanoic (C12:0) or 3-hydroxydodecanoic (C12:0(3-OH)) fatty acyl chain (*m/z* 1136.146 and 1130.813, respectively), or have one pyrophosphoethanolamine group (*m/z* 1129.207) or both a C12:0(3-OH) and a PEA (*m/z* 1089.810) group less. These MS analyses did not provide evidence for the existence of other oligosaccharide glycoforms. Thus, a quantitative truncation of the oligosaccharide chain at the distal Gal residue was produced.

The mass spectra of intact LPS from the *lgtB*$^-$ *pagL*$^+$ mutant cultured in the presence of IPTG showed a major triply charged $[M - 3H]^{3-}$ molecular ion (*m/z* 1171.813) (Fig. 2*B*), which is in agreement with LPS being composed of the following: (i) pentaacyl lipid A species lacking a C12:0(3-OH) fatty acyl chain, as anticipated from the action of the heterologous PagL enzyme, and an additional PEA group as compared with the wild-type lipid A structure of the *lgtB*$^-$ mutant LPS, and (ii) the same L3-immunotype oligosaccharide structure with a truncation of the α chain at the terminal Gal residue, as expected for the inactivation of the *lgtB* gene (see LPS composition proposals in Table 1). In addition to this, a $[M - 3H]^{3-}$ molecular ion of lower abundance (*m/z* 1130.811) (Fig. 2*B*) was displayed, which is consistent with LPS species being substituted with one less PEA group as compared with the main LPS species. Also, three minor $[M - 3H]^{3-}$ molecular ions were observed (*m/z* 1190.821, 1237.865, and 1196.863) (Fig. 2*B*) corresponding to LPS, which, as compared with the main LPS species, have additionally one glycine residue, one more C12:0(3-OH) fatty acyl chain, and the combination of one more C12:0(3-OH) fatty acyl chain and one less PEA group, respectively (Table 1). The total abundance of hexaacylated LPS, as estimated from the relative intensity of their corresponding ion signals (*m/z* 1237.865 and 1196.863) (Fig. 2*B*), was 9%. Thus, minor hexaacylated LPS species were present in this preparation, which would probably have resulted from incomplete LPS 3-*O*-deacylation by the heterologously expressed PagL enzyme. Furthermore, these analyses give further proof of the ability of *N. meningitidis* to decorate LPS with glycine. Previously, other L3 and L4 immunotype strains of *N. meningitidis* have been shown to express LPS molecules with a glycine residue attached at the 7-position of the side-branch heptose in the inner core of LPS (27). Therefore, the *lgtB*$^-$ *pagL*$^+$ mutant LPS displayed a relatively reduced heterogeneity, which was mainly due to the presence of lipid A with two different (3P + 2PEA and 3P + PEA, where P is phosphate) phosphorylation states. Again, the loss of the terminal

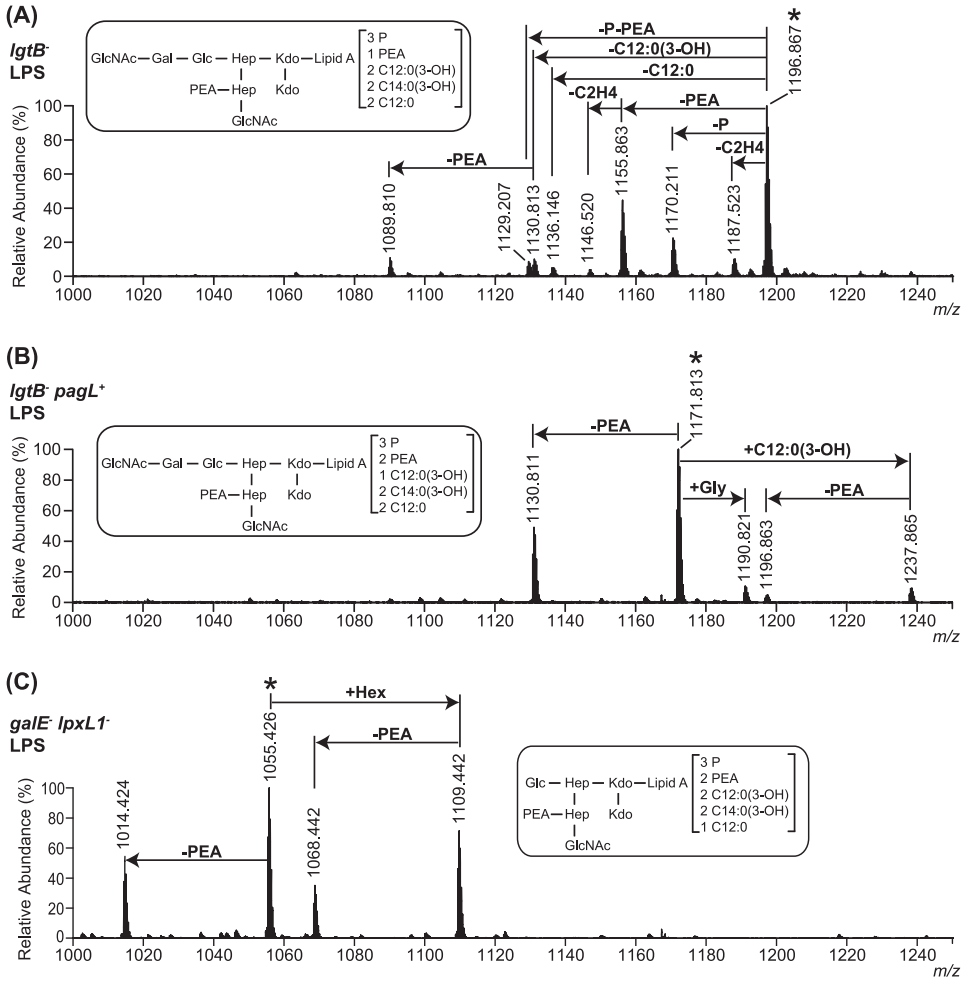

FIGURE 2. **Negative ion ESI-FT-MS of mutant LPS.** The triply charged $[M - 3H]^{3-}$ molecular ion region for the LPS from *lgtB*$^-$ (*A*), *lgtB*$^-$ *pagL*$^+$ (*B*), and *galE*$^-$ *lpxL1*$^-$ (*C*) mutants of *N. meningitidis* is shown. The *insets* contain simplified representations of the LPS structures assigned to base molecular ions (highlighted by *asterisks*). See Table 1 for detailed LPS composition proposals. All annotations refer to the triply charged monoisotopic *m/z* values.

Gal residue, due to the inactivation of the *lgtB* gene in the *lgtB*$^-$ *pagL*$^+$ mutant, was quantitative.

The most prominent signal of the triply charged $[M - 3H]^{3-}$ molecular ion region of the mass spectra of the intact LPS from the *galE*$^-$ *lpxL1*$^-$ mutant (*m/z* 1055.426) (Fig. 2*C*) is in accordance with LPS species consisting of the following: (i) pentaacyl lipid A species substituted with one less C12:0 fatty acyl chain, as can be predicted from the inactivation of the *lpxL1* acyltransferase gene, and an additional PEA group as compared with the wild-type hexaacyl lipid A structure of the *lgtB*$^-$ mutant LPS; and (ii) an L3-immunotype oligosaccharide structure with a truncation of its α chain at the proximal Gal residue, as expected from the inactivation of the *galE* gene (see Table 1 for LPS composition proposals). Other prominent $[M - 3H]^{3-}$ molecular ions (*m/z* 1014.424, 1109.442, and 1068.442) (Fig. 2*C*) were shown that are consistent with LPS structures containing, as compared with the main LPS species, one less PEA, an additional hexose, and the combination of one less PEA and an additional hexose, respectively (Table 1).

Consequently, the structural heterogeneity of the *galE*$^-$ *lpxL1*$^-$ mutant LPS resulted from the combination of two oligosaccharide glycoforms differing in length by one hexose unit and two phosphorylation (3P + 2PEA and 3P + PEA) states of the lipid A. In contrast to the *lgtB*$^-$ and *lgtB*$^-$ *pagL*$^+$ mutant LPS, which showed some degree of heterogeneity in terms of lipid A acylation, the *galE*$^-$ *lpxL1*$^-$ mutant LPS was composed of pentaacyl LPS species exclusively. Interestingly, we observed increased substitution of lipid A with PEA for both pentaacyl forms, which may indicate a compensatory mechanism for the loss of a sixth acyl group.

Fragmentation analysis of the mutant LPS by in-source collision-induced fragmentation generated fragment ions corresponding to the lipid A and oligosaccharide moieties of LPS with *m/z* values that are in agreement with LPS composition proposals described above. SID of the LPS from *lgtB*$^-$ mutant produced doubly deprotonated Y-type fragment ions (*m/z* 957.046, 917.062, and 895.541) accounting for hexaacyl lipid A structures substituted with 3P + PEA, 2P + PEA and 3P, respectively (Fig. 3*A* and Table 2). Furthermore, a singly deprotonated B-type fragment ion was observed (*m/z* 1676.520), which is interpreted as the dehydrated derivative of an L3-immunotype oligosaccharide structure lacking the terminal Gal.

SID fragmentation spectra of the LPS from the *lgtB*$^-$ *pagL*$^+$ mutant contained a major doubly deprotonated Y-type fragment ion (*m/z* 919.468) that is consistent with pentaacyl lipid A species lacking a C12:0(3-OH) fatty acyl chain and containing

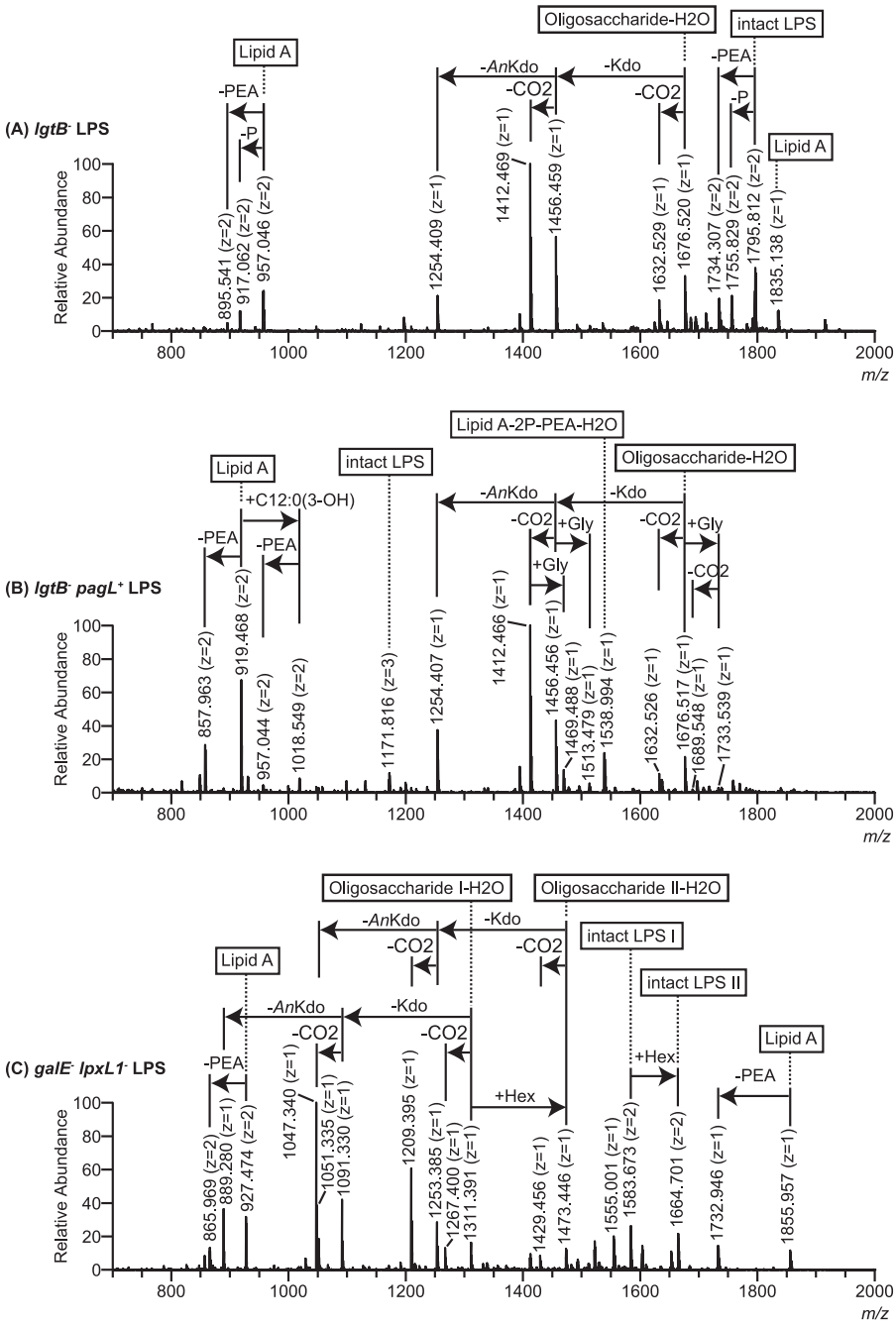

FIGURE 3. **Mass spectrometric fragmentation analysis of mutant LPS.** Negative ion (ESI-FT) in-source collision-induced fragmentation mass spectra of the LPS from *lgtB*$^-$ (*A*), *lgtB*$^-$ *pagL*$^+$ (*B*), and *galE*$^-$ *lpxL1*$^-$ (*C*) mutants of *N. meningitidis*. Negative ion fragments corresponding to lipid A and oligosaccharide domains are depicted. The charge state of ion species is indicated in *parentheses*. See Table 2 for detailed LPS composition.

an additional PEA group, as compared with the wild-type hexaacyl lipid A structure of the *lgtB*$^-$ mutant LPS (Fig. 3*B* and Table 2). Other accompanying doubly deprotonated Y-type fragment ions (*m/z* 857.963, 1018.549, and 957.044) are consistent with lipid A species which, as compared with the major pentaacyl lipid A species, carry one less PEA, an additional C12:0(3-OH) fatty acyl chain, and the combination of one less PEA and an additional C12:0(3-OH) fatty acyl chain, respectively. As shown earlier for the LPS of the *lgtB*$^-$ mutant, fragmentation of the *lgtB*$^-$ *pagL*$^+$ mutant LPS gave proof for the existence of a major oligosaccharide species, which was observed as the dehydrated derivative, as a singly deprotonated B-type fragment ion of *m/z* 1676.517. This is also in accordance with the oligosaccharide having an L3-immunotype structure with a truncation of its α chain at the distal Gal residue. Besides, a singly deprotonated B-type fragment ion of minor abundance (*m/z* 1733.539) was shown corresponding to the dehydrated derivative of the aforementioned oligosaccharide structure being additionally substituted with a glycine residue.

SID fragmentation of the *galE*$^-$ *lpxL1*$^-$ mutant LPS showed a major doubly deprotonated Y-type fragment ion (*m/z* 927.474) consistent with pentaacyl lipid A species containing one less C12:0 fatty acyl chain and an additional PEA group, as compared with the wild-type hexaacyl lipid A structure of the

TABLE 2

Proposed compositions for the negative fragment ions obtained by in-source collision-induced dissociation ESI-FT-MS of the LPS from *lgtB*$^-$, *lgtB*$^-$ *pagL*$^+$, and *galE*$^-$ *lpxL1*$^-$ mutants of *N. meningitidis* (see Fig. 3)

LPS	Ion type [a]	Measured *m/z*	Proposed composition		Calculated *m/z*	Deviation (ppm)
			Oligosaccharide	Lipid A		
lgtB$^-$	$[Y\text{-}2H]^{2-}$	895.541		HexN**2**•P**3**•C_{12}OH**2**•C_{14}OH**2**•C_{12}**2**	895.538	3.1
	$[Y\text{-}2H]^{2-}$	917.062		HexN**2**•P**2**•PEA**1**•C_{12}OH**2**•C_{14}OH**2**•C_{12}**2**	917.059	2.9
	$[Y\text{-}2H]^{2-}$	957.046		HexN**2**•P**3**•PEA**1**•C_{12}OH**2**•C_{14}OH**2**•C_{12}**2**	957.042	3.7
	$[B\text{-}H]^{1-}$	1676.520	Hex**2**•HexNAc**2**•Hep**2**•PEA**1**•Kdo•*An*Kdo		1676.508	7.0
lgtB$^-$ *pagL*$^+$	$[Y\text{-}2H]^{2-}$	857.963		HexN**2**•P**3**•PEA**1**•C_{12}OH**1**•C_{14}OH**2**•C_{12}**2**	857.961	1.8
	$[Y\text{-}2H]^{2-}$	919.468		HexN**2**•P**3**•PEA**2**•C_{12}OH**1**•C_{14}OH**2**•C_{12}**2**	919.466	2.5
	$[Y\text{-}2H]^{2-}$	957.044		HexN**2**•P**3**•PEA**1**•C_{12}OH**2**•C_{14}OH**2**•C_{12}**2**	957.042	1.6
	$[Y\text{-}2H]^{2-}$	1018.549		HexN**2**•P**3**•PEA**2**•C_{12}OH**2**•C_{14}OH**2**•C_{12}**2**	1018.547	2.2
	$[B\text{-}H]^{1-}$	1676.517	Hex**2**•HexNAc**2**•Hep**2**•PEA**1**•Kdo•*An*Kdo		1676.508	5.2
	$[B\text{-}H]^{1-}$	1733.539	Hex**2**•HexNAc**2**• Hep**2**•Gly**1**•PEA**1**•Kdo•*An*Kdo		1733.529	5.6
galE$^-$ *lpxL1*$^-$	$[Y\text{-}2H]^{2-}$	865.969		HexN**2**•P**3**•PEA**1**•C_{12}OH**2**•C_{14}OH**2**•C_{12}**1**	865.959	11.6
	$[Y\text{-}2H]^{2-}$	927.474		HexN**2**•P**3**•PEA**2**•C_{12}OH**2**•C_{14}OH**2**•C_{12}**1**	927.463	11.6
	$[B\text{-}H]^{1-}$	1311.391	Hex**1**•HexNAc**1**•Hep**2**•PEA**1**•Kdo•*An*Kdo		1311.376	11.3
	$[B\text{-}H]^{1-}$	1473.446	Hex**2**•HexNAc**1**•Hep**2**•PEA**1**•Kdo•*An*Kdo		1473.429	11.6

[a] Fragment ions are assigned according to the nomenclature of Domon and Costello (21). Abbreviations used are as follows: Kdo, 3-deoxy-D-*manno*-oct-2-ulosonic acid; *An*Kdo, anhydro-Kdo; Hep, L-*glycero*-D-*manno*-heptose; Hex, hexose; HexN, hexosamine; HexNAc, *N*-acetylhexosamine; Gly, glycine; P, phosphate; C_{12}OH, 3-hydroxydodecanoic acid; C_{14}OH, 3-hydroxytetradecanoic acid; C_{12}, dodecanoic acid.

lgtB$^-$ mutant LPS (Fig. 3*C* and Table 2). This was accompanied by a doubly deprotonated Y-type fragment ion of lower abundance (*m/z* 865.969), which is interpreted as a lipid A structure containing one less PEA as compared with the major pentaacyl lipid A species of this preparation. Furthermore, signals of singly deprotonated B-type fragment ions corresponding to the dehydrated derivatives of an L3-immunotype oligosaccharide structure with truncation of its α chain at the proximal Gal residue and the same structure with an additional hexose were observed (*m/z* 1311.391 and 1473.446, respectively) (Fig. 3*C* and Table 2).

Cytokine Induction in Human Monocytic Cells by Purified Mutant LPS—The bioactivity of purified mutant LPS was determined in the monocytic cell line Mono Mac 6. The capacity of pentaacylated LPS from *lgtB*$^-$ *pagL*$^+$ and *galE*$^-$ *lpxL1*$^-$ mutants to induce the production of the (MyD88-dependent) pro-inflammatory cytokine interleukin-6 (IL-6) differed markedly from that of hexaacylated LPS from the *lgtB*$^-$ mutant (Fig. 4). The production of IL-6 by MM6 cells in response to the stimulation with pentaacyl 3-*O*-deacylated LPS from the *lgtB*$^-$ *pagL*$^+$ mutant (Fig. 4, *squares*) was much lower than that with the hexaacyl LPS from the *lgtB*$^-$ mutant carrying a wild-type lipid A structure (Fig. 4, *circles*), thus indicating much lower toxicity for pentaacyl LPS from the *lgtB*$^-$ *pagL*$^+$ mutant. Strikingly, the LPS from the *galE*$^-$ *lpxL1*$^-$ mutant completely failed to induce the production of IL-6 in MM6 cells at the concentrations used (Fig. 4, *triangles*). Moreover, addition of the pentaacylated LPS from either the *lgtB*$^-$ *pagL*$^+$ or the *galE*$^-$ *lpxL1*$^-$ mutants at an excess weight ratio of 6:1 to the hexaacylated LPS from the *lgtB*$^-$ mutant considerably decreased the IL-6 inducing activity of hexaacylated LPS in MM6 cells (Fig. 5). Hence, these pentaacylated LPS structures not only proved to have weak agonist pro-inflammatory IL-6 inducing activity, but they also were able to antagonize hexaacylated LPS.

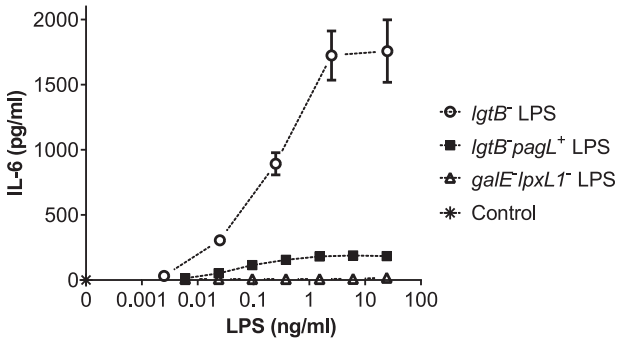

FIGURE 4. **Production of IL-6 by MM6 cells upon incubation with mutant LPS.** MM6 cells were incubated with the indicated concentrations of LPS preparations from *lgtB*$^-$ (*open circle*), *lgtB*$^-$ *pagL*$^+$ (*closed square*), and *galE*$^-$ *lpxL1*$^-$ (*open triangle*) mutants of *N. meningitidis* for 18 h at 37 °C in a 5% CO_2-humidified atmosphere. As control, cells were incubated in supplemented IMDM only (*asterisk*). The concentration of IL-6 in supernatants was determined by ELISA. Data points represent the average of quadruplicate determinations. *Error bars* represent the standard deviation.

The question remained whether the weak IL-6 inducing activity of pentaacylated LPS from the *lgtB*$^-$ *pagL*$^+$ mutant of *N. meningitidis* (Fig. 4, *squares*) was a result of the presence of minor hexaacyl LPS species (Fig. 2*B*, *m/z* 1237.865 and *m/z* 1196.863) in this preparation. Given that 3-*O*-acylated fatty acids in LPS are especially labile to alkaline hydrolysis (28, 29) and to answer this question, we performed a very mild alkaline hydrolysis of the LPS in 5% triethylamine at 45 °C. First, the hexaacylated LPS from the *lgtB*$^-$ mutant was subjected to alkaline hydrolysis under these conditions to determine how specific these were for the cleavage of 3-*O*-acylated C12:0(3-OH) fatty acids. As a result, mass spectra of the LPS from the *lgtB*$^-$

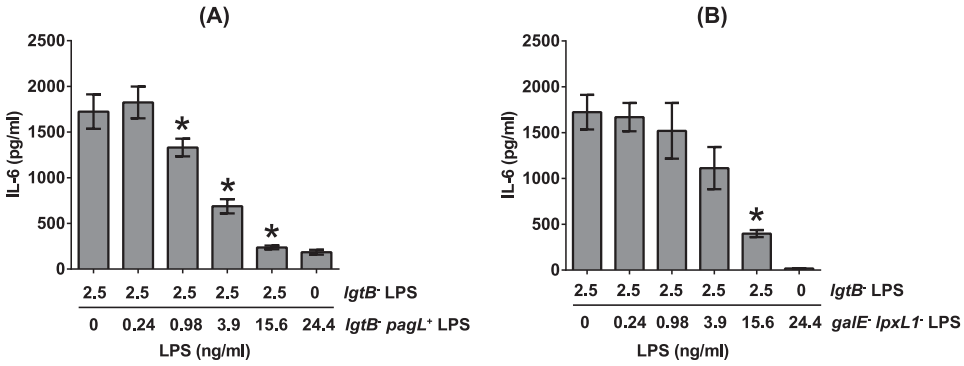

FIGURE 5. **Inhibition of IL-6 inducing activity of hexaacylated LPS from *lgtB*$^-$ mutant in MM6 cells by the pentaacylated LPS from *lgtB*$^-$ *pagL*$^+$ and *galE*$^-$ *lpxL1*$^-$ mutants.** *Asterisks* indicate statistically significant differences ($p < 0.05$) in the level of IL-6 expression between MM6 cells stimulated with *lgtB*$^-$ LPS only and those stimulated with a mixture of *lgtB*$^-$ LPS and *lgtB*$^-$ *pagL*$^+$ LPS (*A*), or between *lgtB*$^-$ LPS only and those stimulated with a mixture of *lgtB*$^-$ LPS and *galE*$^-$ *lpxL1*$^-$ LPS (*B*) as determined by the Mann-Whitney test by using GraphPad Prism 6.0 statistical software (GraphPad Software, Inc.). *Bars* represent the average of quadruplicate determinations and *error bars* the standard deviation.

mutant showed a shift of −198.16 Da as compared with the mass spectra of untreated LPS (data not shown), which is consistent with the cleavage of a single 3-*O*-acylated C12:0(3-OH) fatty acid from LPS. Also, the mass spectra of the LPS from the *lgtB*$^-$ *pagL*$^+$ mutant (Fig. 6*A*) resembled closely those of the same LPS incubated in neutral 5% triethylamine (Fig. 6*B* and Table 3), thus indicating that the procedure used for preparing LPS prior to MS analysis (*e.g.* LPS precipitation with ethanol) did not appreciably affect LPS composition. Finally, mass spectra of the pentaacylated LPS from the *lgtB*$^-$ *pagL*$^+$ mutant after being subjected to mild alkaline hydrolysis showed major signals corresponding to intact pentaacyl 3-*O*-deacylated LPS species (Fig. 6*C*, *m/z* 1171.813 and 1130.810) with minimal degradation (*e.g.* loss of minor species of *m/z* 1190.821 due to the cleavage of the ester-linked glycine group), whereas minor signals of hexaacyl LPS, which were present in the spectra of the untreated LPS from the *lgtB*$^-$ *pagL*$^+$ mutant (Fig. 6*A*, *m/z* 1237.865 and 1196.863), were absent. Then, the bioactivity of this highly pure 3-*O*-deacylated LPS preparation from the *lgtB*$^-$ *pagL*$^+$ mutant was tested in MM6 cells. It was found that the IL-6 inducing activity of these lipopolysaccharides was reduced further after mild alkaline hydrolysis (Fig. 7, *inverted triangles*) but not completely nullified.

Next, the cytokine response induced by mutant LPS preparations in MM6 cells was further characterized by determining the levels produced of the TRIF-dependent chemokine IP-10 (Fig. 8*A*) and the MyD88-dependent anti-inflammatory cytokine IL-10 (Fig. 8*B*). The pentaacylated LPS from the *lgtB*$^-$ *pagL*$^+$ mutant was found to induce lower secretion of IP-10 chemokine (Fig. 8*A*, *squares*) and anti-inflammatory cytokine IL-10 (Fig. 8*B*, *squares*) than the hexaacylated LPS preparation from the *lgtB*$^-$ mutant (Fig. 8, *A* and *B*, *circles*). However, the differences in cytokine induction capacity between the pentaacylated LPS from the *lgtB*$^-$ *pagL*$^+$ mutant and the hexaacylated LPS from the *lgtB*$^-$ mutant were clearly much lower in terms of IP-10 and IL-10 secretion (Fig. 8, *A* and *B*, *squares versus circles*) than in terms of IL-6 production (Fig. 4, *squares versus circles*). Although the IL-10 and IP-10 inducing activities of the LPS from the *lgtB*$^-$ *pagL*$^+$ mutant were decreased further after mild alkaline hydrolysis, these responses remained evidently positive (Fig. 8, *A* and *B*, *inverted triangles*). Again, the bioactivity of mild alkaline-treated LPS from the *lgtB*$^-$ *pagL*$^+$ mutant compared much better with the bioactivity of the hexaacylated LPS of the *lgtB*$^-$ mutant in terms of IL-10 and IP-10 inducing activities (Fig. 8, *A* and *B*, *inverted triangles versus circles*) than in terms of IL-6 inducing activity (Fig. 7, *inverted triangles versus circles*). These results consequently indicate that although the 3-*O*-deacylated LPS from the *lgtB*$^-$ *pagL*$^+$ mutant of *N. meningitidis* has a much lower capacity to induce pro-inflammatory effects *in vitro,* it is still capable of activating human innate immune cells. In contrast, the LPS from the *galE*$^-$ *lpxL1*$^-$ mutant was at the concentrations used also devoid of IL-10 and IP-10 inducing activity in MM6 cells (Fig. 8, *diamonds*).

DISCUSSION

Modification of LPS biosynthesis offers the potential to create many different variant molecules that are more suitable for inclusion in vaccines because of reduced toxicity. Such novel variants can be used as intrinsic adjuvants in *e.g.* outer membrane vesicle or whole cell vaccines or as external adjuvants formulated with more purified antigens. In both cases, it is essential to have methods for the complete structural characterization of the resulting LPS variants, as biosynthesis and modification steps can be incomplete and may lead to complicated mixtures that are difficult to reproduce. We have obtained a derivative of the meningococcal strain H44/76 carrying the PagL lipid A 3-*O*-deacylase from *B. bronchiseptica* and with the lipopolysaccharide glycosyltransferase B inactivated. High resolution mass spectrometry was used to fully characterize the molecular composition and heterogeneity of intact LPS. We found that the LPS produced is mainly composed of pentaacylated molecular species, lacking a C12:0(3-OH) fatty acyl chain and carrying three phosphates and one or two PEA groups in the lipid A. Although hexaacylated LPS species were also present, these were only of minor abundance. Consequently, a high efficiency of conversion of the wild-type hexaacyl to the 3-*O*-deacyl pentaacyl LPS form was achieved by the heterologous expression of the PagL enzyme. Because lipid A-modifying enzymes like PagL and PagP often only converse a fraction of the total LPS, they may increase LPS heterogeneity; in addition, some modifications may trigger secondary alterations that further complicate the final composi-

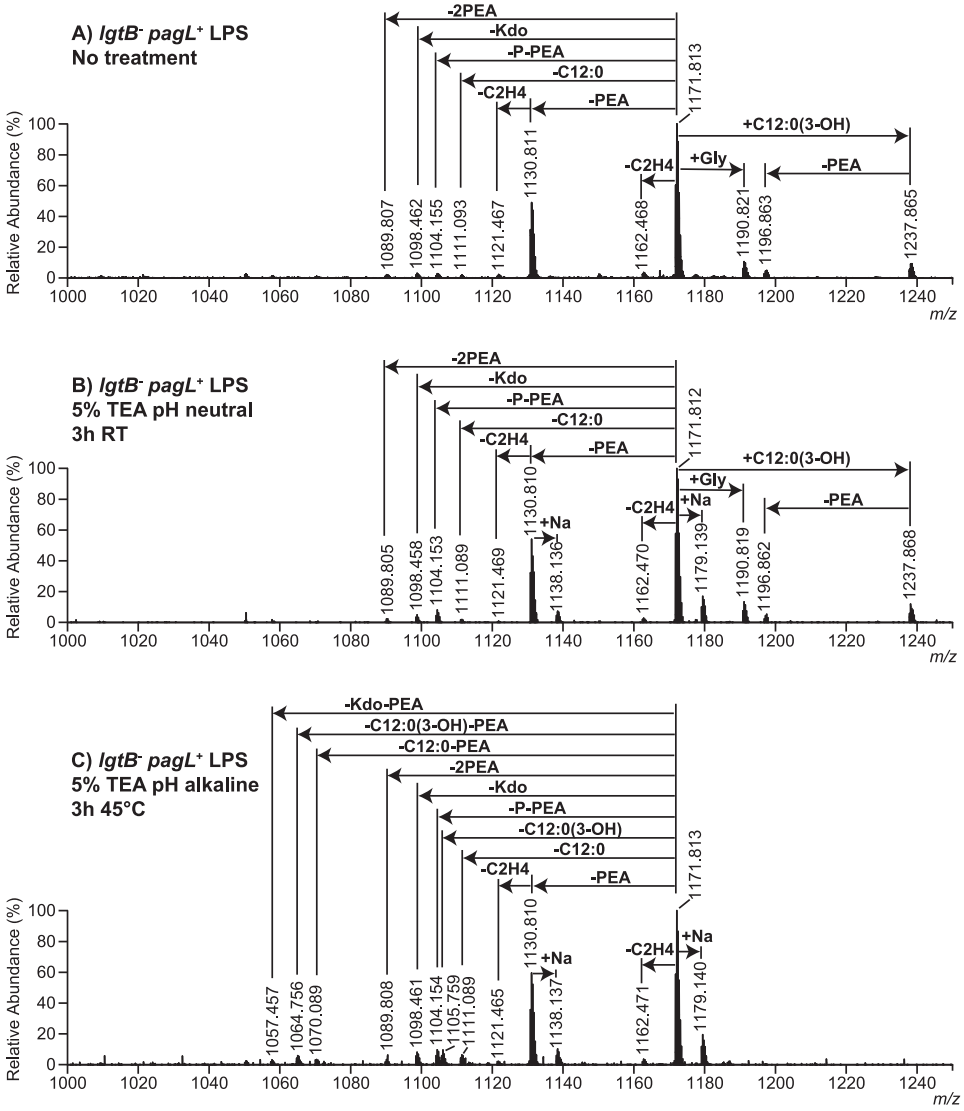

FIGURE 6. **Negative ion ESI-FT-MS of LPS from the *lgtB*$^-$ *pagL*$^+$ mutant of *N. meningitidis* after mild alkaline hydrolysis.** The triply charged $[M - 3H]^{3-}$ molecular ion regions of the mass spectra of untreated LPS (*A*), LPS that had been incubated in neutral 5% TEA at RT for 3 h (*B*), and LPS that had been incubated in 5% alkaline triethylamine at 45 °C for 3 h (*C*) are presented. LPS composition proposals are shown in Table 3. The charge state of annotated molecular ions is $z = 3$.

tion (10, 30). This can be a complicating factor when analyzing the biological effect of the introduced modifications, as the mixtures may have different properties compared with their individual constituents. The nearly complete deacylation we observed for the *B. bronchiseptica* PagL working on meningococcal LPS is therefore advantageous. MS analyses provided evidence for the expression of only one major oligosaccharide glycoform lacking the terminal Gal residue, which is in agreement with an effective inactivation of the *lgtB* glycosyltransferase gene. Phase variable expression of *lgtA* might conceivably have led to oligosaccharide heterogeneity (31), through loss of the terminal GlcNAc residue in the *lgtB* mutant strain, but our structural data showed this not to be the case. Consequently, the heterogeneity of the LPS obtained was relatively minor. This is advantageous when considering the potential application of this LPS as a vaccine adjuvant because this will facilitate LPS quality control and more reproducible manufacturing of LPS preparations.

Although the lipid A moiety is the primary determinant of LPS biological activity, the oligosaccharide region can also play an important role. First, it increases solubility of LPS, which is convenient when developing a production process suitable for clinical grade material. Importantly, the *lgtB*$^-$ *pagL*$^+$ LPS was sufficiently water-soluble to allow sterilization through a 0.2-μm filter. Second, the oligosaccharide can be used for targeting to other receptors on immune cells. For this reason, we combined the PagL-deacylated lipid A with *lgtB*$^-$ truncated oligosaccharide, which can bind to the C-type lectin DC-SIGN. Targeting to DC-SIGN could be used to further improve LPS adjuvant properties, as it has been demonstrated to lead to a Th1 bias in T cells activated by *N. meningitidis*-stimulated DC (26). Simultaneous triggering of DC-SIGN and TLR4 could result in cross-presentation and enhanced $CD8^+$ in addition to $CD4^+$ T cell responses (32). It is therefore important that MS analysis of the *lgtB*$^-$ *pagL*$^+$ LPS showed only a single oligosac-

TABLE 3

Proposed compositions for the triply charged $[M - 3H]^{3-}$ molecular ions observed in the ESI-FT-MS of intact LPS from the *lgtB*$^-$ *pagL*$^+$ mutant (Fig. 6*A*, untreated LPS) or of LPS from the *lgtB*$^-$ *pagL*$^+$ mutant incubated either in neutral 5% TEA at RT (Fig. 6*B*) or in alkaline 5% TEA at 45 °C (Fig. 6*C*)

Figure	Ion type	Measured *m/z*	Proposed LPS composition		Calculated *m/z*	Deviation (ppm)
			Oligosaccharide	Lipid A		
Fig. 6A	$[M-3H]^{3-}$	1089.807	Hex**2**•HexNAc**2**• Hep**2**•PEA**1**•Kdo**2**	HexN**2**•P**3**•C_{12}OH**1**•C_{14}OH**2**•C_{12}**2**	1089.808	0.5
	$[M-3H]^{3-}$	1098.462	Hex**2**•HexNAc**2**• Hep**2**•PEA**1**•Kdo**1**	HexN**2**•P**3**•PEA**2**•C_{12}OH**1**•C_{14}OH**2**•C_{12}**2**	1098.460	1.4
	$[M-3H]^{3-}$	1104.155	Hex**2**•HexNAc**2**• Hep**2**•PEA**1**•Kdo**2**	HexN**2**•P**2**•PEA**1**•C_{12}OH**1**•C_{14}OH**2**•C_{12}**2**	1104.155	0.0
	$[M-3H]^{3-}$	1111.093	Hex**2**•HexNAc**2**• Hep**2**•PEA**1**•Kdo**2**	HexN**2**•P**3**•PEA**2**•C_{12}OH**1**•C_{14}OH**2**•C_{12}**1**	1111.091	1.9
	$[M-3H]^{3-}$	1121.467	Hex**2**•HexNAc**2**• Hep**2**•PEA**1**•Kdo**2**	HexN**2**•P**3**•PEA**1**•C_{12}OH**1**•C_{14}OH**2**•C_{12}**2** -C_2H_4	1121.467	0.3
	$[M-3H]^{3-}$	1130.811	Hex**2**•HexNAc**2**• Hep**2**•PEA**1**•Kdo**2**	HexN**2**•P**3**•PEA**1**•C_{12}OH**1**•C_{14}OH**2**•C_{12}**2**	1130.810	0.5
	$[M-3H]^{3-}$	1162.468	Hex**2**•HexNAc**2**• Hep**2**•PEA**1**•Kdo**2**	HexN**2**•P**3**•PEA**2**•C_{12}OH**1**•C_{14}OH**2**•C_{12}**2** -C_2H_4	1162.469	1.3
	$[M-3H]^{3-}$	1171.813	Hex**2**•HexNAc**2**• Hep**2**•PEA**1**•Kdo**2**	HexN**2**•P**3**•PEA**2**•C_{12}OH**1**•C_{14}OH**2**•C_{12}**2**	1171.813	0.2
	$[M-3H]^{3-}$	1190.821	Hex**2**•HexNAc**2**• Hep**2**•Gly**1**•PEA**1**•Kdo**2**	HexN**2**•P**3**•PEA**2**•C_{12}OH**1**•C_{14}OH**2**•C_{12}**2**	1190.820	0.5
	$[M-3H]^{3-}$	1196.863	Hex**2**•HexNAc**2**• Hep**2**•PEA**1**•Kdo**2**	HexN**2**•P**3**•PEA**1**•C_{12}OH**2**•C_{14}OH**2**•C_{12}**2**	1196.864	1.2
	$[M-3H]^{3-}$	1237.865	Hex**2**•HexNAc**2**• Hep**2**•PEA**1**•Kdo**2**	HexN**2**•P**3**•PEA**2**•C_{12}OH**2**•C_{14}OH**2**•C_{12}**2**	1237.867	1.8
Fig. 6B	$[M-3H]^{3-}$	1089.805	Hex**2**•HexNAc**2**• Hep**2**•PEA**1**•Kdo**2**	HexN**2**•P**3**•C_{12}OH**1**•C_{14}OH**2**•C_{12}**2**	1089.808	2.3
	$[M-3H]^{3-}$	1098.458	Hex**2**•HexNAc**2**• Hep**2**•PEA**1**•Kdo**1**	HexN**2**•P**3**•PEA**2**•C_{12}OH**1**•C_{14}OH**2**•C_{12}**2**	1098.460	2.3
	$[M-3H]^{3-}$	1104.153	Hex**2**•HexNAc**2**• Hep**2**•PEA**1**•Kdo**2**	HexN**2**•P**2**•PEA**1**•C_{12}OH**1**•C_{14}OH**2**•C_{12}**2**	1104.155	1.8
	$[M-3H]^{3-}$	1111.089	Hex**2**•HexNAc**2**• Hep**2**•PEA**1**•Kdo**2**	HexN**2**•P**3**•PEA**2**•C_{12}OH**1**•C_{14}OH**2**•C_{12}**1**	1111.091	1.7
	$[M-3H]^{3-}$	1121.469	Hex**2**•HexNAc**2**• Hep**2**•PEA**1**•Kdo**2**	HexN**2**•P**3**•PEA**1**•C_{12}OH**1**•C_{14}OH**2**•C_{12}**2** -C_2H_4	1121.467	2.1
	$[M-3H]^{3-}$	1130.810	Hex**2**•HexNAc**2**• Hep**2**•PEA**1**•Kdo**2**	HexN**2**•P**3**•PEA**1**•C_{12}OH**1**•C_{14}OH**2**•C_{12}**2**	1130.810	0.3
	$[M-4H+Na]^{3-}$	1138.136	Hex**2**•HexNAc**2**• Hep**2**•PEA**1**•Kdo**2**	HexN**2**•P**3**•PEA**1**•C_{12}OH**1**•C_{14}OH**2**•C_{12}**2**	1138.138	1.3
	$[M-3H]^{3-}$	1162.470	Hex**2**•HexNAc**2**• Hep**2**•PEA**1**•Kdo**2**	HexN**2**•P**3**•PEA**2**•C_{12}OH**1**•C_{14}OH**2**•C_{12}**2** -C_2H_4	1162.469	0.5
	$[M-3H]^{3-}$	1171.812	Hex**2**•HexNAc**2**• Hep**2**•PEA**1**•Kdo**2**	HexN**2**•P**3**•PEA**2**•C_{12}OH**1**•C_{14}OH**2**•C_{12}**2**	1171.813	1.1
	$[M-4H+Na]^{3-}$	1179.139	Hex**2**•HexNAc**2**• Hep**2**•PEA**1**•Kdo**2**	HexN**2**•P**3**•PEA**2**•C_{12}OH**1**•C_{14}OH**2**•C_{12}**2**	1179.140	1.2
	$[M-3H]^{3-}$	1190.819	Hex**2**•HexNAc**2**• Hep**2**•Gly**1**•PEA**1**•Kdo**2**	HexN**2**•P**3**•PEA**2**•C_{12}OH**1**•C_{14}OH**2**•C_{12}**2**	1190.820	1.2
	$[M-3H]^{3-}$	1196.862	Hex**2**•HexNAc**2**• Hep**2**•PEA**1**•Kdo**2**	HexN**2**•P**3**•PEA**1**•C_{12}OH**2**•C_{14}OH**2**•C_{12}**2**	1196.864	2.0
	$[M-3H]^{3-}$	1237.868	Hex**2**•HexNAc**2**• Hep**2**•PEA**1**•Kdo**2**	HexN**2**•P**3**•PEA**2**•C_{12}OH**2**•C_{14}OH**2**•C_{12}**2**	1237.867	0.6
Fig. 6C	$[M-3H]^{3-}$	1057.457	Hex**2**•HexNAc**2**• Hep**2**•PEA**1**•Kdo**1**	HexN**2**•P**3**•PEA**1**•C_{12}OH**1**•C_{14}OH**2**•C_{12}**2**	1057.458	0.6
	$[M-3H]^{3-}$	1064.756	Hex**2**•HexNAc**2**• Hep**2**•PEA**1**•Kdo**2**	HexN**2**•P**3**•PEA**1**•C_{14}OH**2**•C_{12}**2**	1064.756	0.4
	$[M-3H]^{3-}$	1070.089	Hex**2**•HexNAc**2**• Hep**2**•PEA**1**•Kdo**2**	HexN**2**•P**3**•PEA**1**•C_{12}OH**1**•C_{14}OH**2**•C_{12}**1**	1070.088	0.9
	$[M-3H]^{3-}$	1089.808	Hex**2**•HexNAc**2**• Hep**2**•PEA**1**•Kdo**2**	HexN**2**•P**3**•C_{12}OH**1**•C_{14}OH**2**•C_{12}**2**	1089.808	0.4
	$[M-3H]^{3-}$	1098.461	Hex**2**•HexNAc**2**• Hep**2**•PEA**1**•Kdo**1**	HexN**2**•P**3**•PEA**2**•C_{12}OH**1**•C_{14}OH**2**•C_{12}**2**	1098.460	0.5
	$[M-3H]^{3-}$	1104.154	Hex**2**•HexNAc**2**• Hep**2**•PEA**1**•Kdo**2**	HexN**2**•P**2**•PEA**1**•C_{12}OH**1**•C_{14}OH**2**•C_{12}**2**	1104.155	0.9
	$[M-3H]^{3-}$	1105.759	Hex**2**•HexNAc**2**• Hep**2**•PEA**1**•Kdo**2**	HexN**2**•P**3**•PEA**2**•C_{14}OH**2**•C_{12}**2**	1105.759	0.2
	$[M-3H]^{3-}$	1111.089	Hex**2**•HexNAc**2**• Hep**2**•PEA**1**•Kdo**2**	HexN**2**•P**3**•PEA**2**•C_{12}OH**1**•C_{14}OH**2**•C_{12}**1**	1111.091	1.7
	$[M-3H]^{3-}$	1121.465	Hex**2**•HexNAc**2**• Hep**2**•PEA**1**•Kdo**2**	HexN**2**•P**3**•PEA**1**•C_{12}OH**1**•C_{14}OH**2**•C_{12}**2** -C_2H_4	1121.467	1.4
	$[M-3H]^{3-}$	1130.810	Hex**2**•HexNAc**2**• Hep**2**•PEA**1**•Kdo**2**	HexN**2**•P**3**•PEA**1**•C_{12}OH**1**•C_{14}OH**2**•C_{12}**2**	1130.810	0.3
	$[M-4H+Na]^{3-}$	1138.137	Hex**2**•HexNAc**2**• Hep**2**•PEA**1**•Kdo**2**	HexN**2**•P**3**•PEA**1**•C_{12}OH**1**•C_{14}OH**2**•C_{12}**2**	1138.138	0.5
	$[M-3H]^{3-}$	1162.471	Hex**2**•HexNAc**2**• Hep**2**•PEA**1**•Kdo**2**	HexN**2**•P**3**•PEA**2**•C_{12}OH**1**•C_{14}OH**2**•C_{12}**2** -C_2H_4	1162.469	1.3
	$[M-3H]^{3-}$	1171.813	Hex**2**•HexNAc**2**• Hep**2**•PEA**1**•Kdo**2**	HexN**2**•P**3**•PEA**2**•C_{12}OH**1**•C_{14}OH**2**•C_{12}**2**	1171.813	0.2
	$[M-4H+Na]^{3-}$	1179.140	Hex**2**•HexNAc**2**• Hep**2**•PEA**1**•Kdo**2**	HexN**2**•P**3**•PEA**2**•C_{12}OH**1**•C_{14}OH**2**•C_{12}**2**	1179.140	0.3

charide glycoform with the structure required for DC-SIGN binding, *i.e.* without the terminal Gal residue due to *lgtB* mutation.

The LPS from the *galE*$^-$ *lpxL1*$^-$ mutant showed oligosaccharide heterogeneity consisting of two glycoforms differing in length by one hexose unit. According to the general L3-immu-

notype oligosaccharide structure (Fig. 1*A*), the additional hexose residue would correspond to galactose. However, this seems unlikely because the *galE* gene was inactivated in this bacterial mutant, and therefore, these bacteria are unable to incorporate galactose. Alternatively, the existence of LPS species with an additional hexose may indicate some relaxation of the substrate specificity of the lipopolysaccharide glycosyltransferase E, which adds the first galactose of the lacto-*N*-tetraose chain Gal-GlcNAc-Gal-Glc in LPS (Fig. 1*A*), because LPS structures with a second glucose residue, in replacement of galactose, have been observed previously in other *galE*$^-$ mutants of *N. meningitidis* (33, 34). The introduction of the *galE*$^-$ mutation in the LPS has the advantage that, similarly to the *lgtB*$^-$ mutation, it disrupts the lacto-*N*-tetraose unit of the oligosaccharide, which could potentially lead to an immune response against self-antigens in humans, thus eliminating this risk (35). The *galE* oligosaccharide truncation, however, is not known to provide any improvement in terms of targeting to carbohydrate-binding receptors in professional immune cells such as DC-SIGN in human DC cells (26).

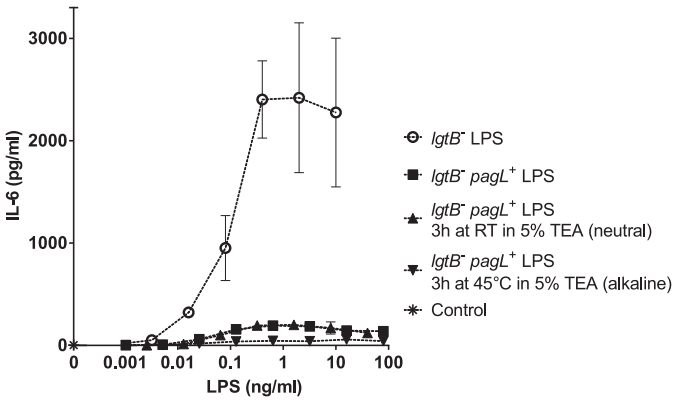

FIGURE 7. **Effect of mild alkaline hydrolysis on the capacity of LPS from *lgtB*$^-$ *pagL*$^+$ meningococci to induce the secretion of IL-6 in MM6 cells.** The production of IL-6 by MM6 cells stimulated with serial dilutions of LPS from the *lgtB*$^-$ mutant (*open circles*) and the *lgtB*$^-$ *pagL*$^+$ mutant of *N. meningitidis,* which had been left untreated (*squares*), incubated in neutral 5% TEA at RT for 3 h (*triangles*) or incubated in alkaline 5% TEA at 45 °C for 3 h (*inverted triangles*) is shown. As control, cells were incubated without LPS in supplemented IMDM (*asterisk*). IL-6 concentration in supernatants was determined by ELISA. Results are the average of quadruplicate determinations. *Error bars* represent the standard deviation.

In this work, we aimed at evaluating and comparing the effect of *pagL*$^+$ and *lpxL1*$^-$ lipid A mutations on the immunostimulating properties of the LPS of *N. meningitidis*. Toward this end, the LPS from *lgtB*$^-$ *pagL*$^+$ and *galE*$^-$ *lpxL1*$^-$ meningococci were assayed for cytokine induction in the human monocytic cell line MM6. Because MM6 cells do not express DC-SIGN (36), in contrast to human DC cells, they are not expected to react differently to LPS carrying an *lgtB* oligosaccharide truncation. In fact, the presence of *lgtB*$^-$ or *galE*$^-$ oligosaccharide mutations does not influence cytokine response in MM6 cells to hexaacylated LPS (data not shown). Thus, even though the LPS tested also differed in oligosaccharide composition, in this assay system the differences in the response to the LPS were directly attributable to the LPS modifications located in the lipid A moiety.

The functional roles of *lgtB*$^-$ and *galE*$^-$ oligosaccharide mutations with regard to the immunopotentiating properties of LPS have been addressed recently in a separate study in human dendritic cells using OMVs obtained from *N. meningitidis* mutants. It has been shown that *lgtB* oligosaccharide truncation can significantly increase internalization of OMVs by human dendritic cells as compared with wild-type or *galE* truncated oligosaccharides (37). Moreover, the presence of *lgtB* truncated oligosaccharide in OMVs improved human DC maturation, IL-10, and interleukin-23 production by human DC and increased Th17 cell expansion (37). These results suggest that *lgtB* mutation could be a promising approach to enhance antigen-specific immunity.

Although activation of innate immune cells by LPS is central for adjuvant activity, a high level of expression of pro-inflammatory cytokines is undesirable as this leads to high toxicity. It has been suggested that the relatively reduced toxicity and retained adjuvant activity of monophosphoryl lipid A lacking the 1-phosphate are linked to its ability of biasing the activation of TLR4 toward the TRIF-dependent signaling pathway (38). We have described previously that the pentaacylated LPS from an *lpxL1*$^-$ mutant of *N. meningitidis*, lacking the secondary C12:0 acyl chain at the 2′-position of lipid A, has reduced endotoxicity but similar adjuvant activity in mice as compared with wild-type meningococcal LPS (14, 39). However, the *lpxL1*$^-$ LPS was more strongly reduced in its ability to activate human as compared with murine TLR4, as measured by the expression

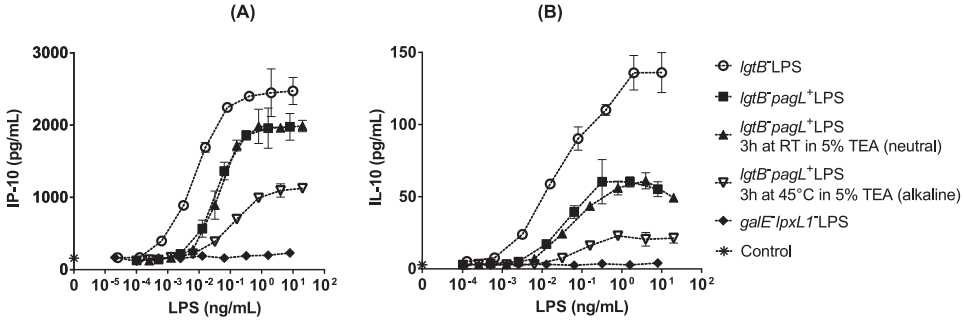

FIGURE 8. **Secretion of IP-10 (*A*) and IL-10 (*B*) by MM6 cells after stimulation with mutant LPS of *N. meningitidis*.** MM6 cells were stimulated with serial dilutions of LPS preparations from the *lgtB*$^-$ (*open circles*), *lgtB*$^-$ *pagL*$^+$ (*closed squares*), or *galE*$^-$ *lpxL1*$^-$ (*closed diamonds*) mutants or of LPS from the *lgtB*$^-$ *pagL*$^+$ mutant that had been previously incubated in neutral 5% TEA at RT for 3 h (*closed triangles*) or subjected to mild alkaline hydrolysis in 5% TEA at 45 °C for 3 h (*open inverted triangles*). Control cells were incubated in supplemented IMDM only (*asterisks*). Cell incubations were performed for 16–18 h at 37 °C in a 5% CO_2-humidified atmosphere. IP-10 and IL-10 concentrations in supernatants were determined by ELISA. Each data point represents the average of triplicate determinations; *error bars* indicate the standard deviation.

of the NF-κB transcription factor and various MyD88-dependent cytokines (40). For PagL-deacylated meningococcal LPS, adjuvant activity has also been demonstrated in mice, but it should be noted that in this animal species there is very little difference in endotoxic activity compared with wild-type hexaacylated LPS (41). In this study, we have determined that the *lpxL1*$^-$-pentaacylated LPS structure containing a fully phosphorylated lipid A, as determined by MS analysis, at the concentrations used is unable to induce the production of not only MyD88-dependent cytokines (IL-6 and IL-10) but also of the TRIF-dependent chemokine IP-10 in human monocytic MM6 cells. This further indicates that *lpxL1*$^-$ LPS may have low immunomodulating activity in humans.

We have shown that a different form of pentaacylated LPS from *N. meningitidis*, the *lgtB*$^-$ *pagL*$^+$ LPS lacking the ester-linked C12:0(3-OH) fatty acyl chain at position 3 of lipid A and containing the same level of lipid A phosphorylation as that of *lpxL1*$^-$ LPS, behaves differently from *lpxL1*$^-$ LPS in terms of innate immune activation capacity, especially with regard to the activation of the TRIF-dependent pathway. The *lgtB*$^-$ *pagL*$^+$ LPS can induce dose-dependent expression of the MyD88-dependent cytokine IL-10, a low level of the MyD88-dependent pro-inflammatory cytokine IL-6 and relatively higher levels of the TRIF-dependent chemokine IP-10 in human monocytic cells. The retained capacity of pentaacylated *lgtB*$^-$ *pagL*$^+$ LPS to induce the secretion of the chemokine IP-10 suggests a bias toward the TRIF over the MyD88 signaling pathway after TLR4 activation, which is considered to be favorable for the development of adaptive immunity (42–45). These results indicate a greater potential of the use of *pagL*$^+$ LPS as compared with *lpxL1*$^-$ LPS for immune potentiation in humans. In addition, they underscore the importance of detailed structure-function analyses of modified LPS species, as even minor differences, like the loss of an acyl chain from either the 2′- or 3-position in the *lpxL1*$^-$ and *pagL*$^+$ strains, respectively, can have differential effects on the TLR4 agonistic activity.

To determine the contribution of minor hexaacylated species to the bioactivity of the LPS from *lgtB*$^-$ *pagL*$^+$ *N. meningitidis*, we have performed mild alkaline hydrolysis to selectively remove 3-*O*-acylated fatty acids from LPS. As a result, highly pure 3-*O*-deacylated LPS species from *lgtB*$^-$ *pagL*$^+$ *N. meningitidis* was obtained, as demonstrated by mass spectrometry analysis. It was found that the IL-6 induction capacity of LPS in human monocytic cells was reduced even further after mild alkaline hydrolysis. However, the stimulating activity of LPS in terms of IP-10 and IL-10 secretion decreased to a much lower extent. Based on these results, it is clear that even in minor amounts of hexaacylated LPS species present in *lgtB*$^-$ *pagL*$^+$ LPS could effectively potentiate the stimulatory capacity of this mostly pentaacylated LPS preparation. It is noteworthy, however, that the immunostimulatory enhancement produced by minor hexaacylated LPS occurred to a level lower than that expected from a simple additive effect due to the competitive inhibition of hexaacylated forms by major pentaacylated LPS species. Most importantly, these results demonstrate that pure and fully 3-*O*-deacylated LPS from *lgtB*$^-$ *pagL*$^+$ *N. meningitidis* has itself substantial immune stimulating activity. Although the relevance in terms of toxicity and adjuvant activity of residual hexaacylated species in *lgtB*$^-$ *pagL*$^+$ LPS mixtures remains to be determined *in vivo*, one may expect that mixtures with specific ratios of hexa- and pentaacylated species could strike an optimal balance between toxicity and adjuvant activity.

In view of the usual presence of minor wild-type LPS species in genetically detoxified LPS mixtures and considering the potential immune modulating effect of this LPS fraction, the present work shows the importance of a careful characterization and separation of all LPS molecular species for a better definition and use of LPS immune stimulating activities.

REFERENCES

1. Miyake, K. (2004) Innate recognition of lipopolysaccharide by Toll-like receptor 4-MD-2. *Trends Microbiol.* **12,** 186–192
2. Raetz, C. R., Reynolds, C. M., Trent, M. S., and Bishop, R. E. (2007) Lipid A modification systems in Gram-negative bacteria. *Annu. Rev. Biochem.* **76,** 295–329
3. Maeshima, N., and Fernandez, R. C. (2013) Recognition of lipid A variants by the TLR4-MD-2 receptor complex. *Front. Cell. Infect. Microbiol.* **3,** 3
4. Brandtzaeg, P., and van Deuren, M. (2002) Current concepts in the role of the host response in *Neisseria meningitidis* septic shock. *Curr. Opin. Infect. Dis.* **15,** 247–252
5. Fransen, F., Heckenberg, S. G., Hamstra, H. J., Feller, M., Boog, C. J., van Putten, J. P., van de Beek, D., van der Ende, A., and van der Ley, P. (2009) Naturally occurring lipid A mutants in *Neisseria meningitidis* from patients with invasive meningococcal disease are associated with reduced coagulopathy. *PLoS Pathog.* **5,** e1000396
6. Holst, J., Martin, D., Arnold, R., Huergo, C. C., Oster, P., O'Hallahan, J., and Rosenqvist, E. (2009) Properties and clinical performance of vaccines containing outer membrane vesicles from *Neisseria meningitidis*. *Vaccine* **27,** Suppl. 2, B3-B12
7. Sanders, H., and Feavers, I. M. (2011) Adjuvant properties of meningococcal outer membrane vesicles and the use of adjuvants in *Neisseria meningitidis* protein vaccines. *Expert Rev. Vaccines* **10,** 323–334
8. van der Ley, P., and van den Dobbelsteen, G. (2011) Next-generation outer membrane vesicle vaccines against *Neisseria meningitidis* based on non-toxic LPS mutants. *Hum. Vaccin.* **7,** 886–890
9. Trent, M. S., Pabich, W., Raetz, C. R., and Miller, S. I. (2001) A PhoP/PhoQ-induced Lipase (PagL) that catalyzes 3-*O*-deacylation of lipid A precursors in membranes of *Salmonella typhimurium*. *J. Biol. Chem.* **276,** 9083–9092
10. Geurtsen, J., Steeghs, L., Hove, J. T., van der Ley, P., and Tommassen, J. (2005) Dissemination of lipid A deacylases (pagL) among Gram-negative bacteria: identification of active-site histidine and serine residues. *J. Biol. Chem.* **280,** 8248–8259
11. Geurtsen, J., Steeghs, L., Hamstra, H. J., Ten Hove, J., de Haan, A., Kuipers, B., Tommassen, J., and van der Ley, P. (2006) Expression of the lipopolysaccharide-modifying enzymes PagP and PagL modulates the endotoxic activity of *Bordetella pertussis*. *Infect. Immun.* **74,** 5574–5585
12. Baart, G. J., de Jong, G., Philippi, M., van't Riet, K., van der Pol, L. A., Beuvery, E. C., Tramper, J., and Martens, D. E. (2007) Scale-up for bulk production of vaccine against meningococcal disease. *Vaccine* **25,** 6399–6408
13. van der Ley, P., van der Biezen, J., and Poolman, J. T. (1995) Construction of *Neisseria meningitidis* strains carrying multiple chromosomal copies of the porA gene for use in the production of a multivalent outer membrane vesicle vaccine. *Vaccine* **13,** 401–407
14. van der Ley, P., Steeghs, L., Hamstra, H. J., ten Hove, J., Zomer, B., and van Alphen, L. (2001) Modification of lipid A biosynthesis in *Neisseria meningitidis* lpxL mutants: influence on lipopolysaccharide structure, toxicity, and adjuvant activity. *Infect. Immun.* **69,** 5981–5990
15. Westphal, O., and Jann, K. (1965) in *Methods in Carbohydrate Chemistry* (Whistler, R. L., and Wolfan, M. L., eds) pp. 83–91, Academic Press, Inc., New York
16. Peterson, G. L. (1983) Determination of total protein. *Methods Enzymol.* **91,** 95–119

17. Bonasera, V., Alberti, S., and Sacchetti, A. (2007) Protocol for high-sensitivity/long linear-range spectrofluorimetric DNA quantification using ethidium bromide. *BioTechniques* **43,** 173–174
18. Karkhanis, Y. D., Zeltner, J. Y., Jackson, J. J., and Carlo, D. J. (1978) A new and improved microassay to determine 2-keto-3-deoxyoctonate in lipopolysaccharide of Gram-negative bacteria. *Anal. Biochem.* **85,** 595–601
19. Kondakov, A., and Lindner, B. (2005) Structural characterization of complex bacterial glycolipids by Fourier transform mass spectrometry. *Eur. J. Mass Spectrom.* **11,** 535–546
20. Wilm, M. S., and Mann, M. (1994) Electrospray and Taylor-Cone theory, Dole's beam of macromolecules at last? *Int. J. Mass Spectrom. Ion. Proc.* **136,** 167–180
21. Domon, B., and Costello, C. E. (1988) A systematic nomenclature for carbohydrate fragmentations in FAB-MS/MS spectra of glycoconjugates. *Glycoconj. J.* **5,** 397–409
22. Maass, K., Ranzinger, R., Geyer, H., von der Lieth, C. W., and Geyer, R. (2007) "Glyco-peakfinder"–*de novo* composition analysis of glycoconjugates. *Proteomics* **7,** 4435–4444
23. Pavliak, V., Brisson, J. R., Michon, F., Uhrín, D., and Jennings, H. J. (1993) Structure of the sialylated L3 lipopolysaccharide of *Neisseria meningitidis*. *J. Biol. Chem.* **268,** 14146–14152
24. van der Ley, P., Kramer, M., Martin, A., Richards, J. C., and Poolman, J. T. (1997) Analysis of the icsBA locus required for biosynthesis of the inner core region from *Neisseria meningitidis* lipopolysaccharide. *FEMS Microbiol. Lett.* **146,** 247–253
25. Ziegler-Heitbrock, H. W., Thiel, E., Fütterer, A., Herzog, V., Wirtz, A., and Riethmüller, G. (1988) Establishment of a human cell line (Mono Mac 6) with characteristics of mature monocytes. *Int. J. Cancer* **41,** 456–461
26. Steeghs, L., van Vliet, S. J., Uronen-Hansson, H., van Mourik, A., Engering, A., Sanchez-Hernandez, M., Klein, N., Callard, R., van Putten, J. P., van der Ley, P., van Kooyk, Y., and van de Winkel, J. G. (2006) *Neisseria meningitidis* expressing lgtB lipopolysaccharide targets DC-SIGN and modulates dendritic cell function. *Cell. Microbiol.* **8,** 316–325
27. Cox, A. D., Li, J., and Richards, J. C. (2002) Identification and localization of glycine in the inner core lipopolysaccharide of *Neisseria meningitidis*. *Eur. J. Biochem.* **269,** 4169–4175
28. Basu, S. S., White, K. A., Que, N. L., and Raetz, C. R. (1999) A deacylase in *Rhizobium leguminosarum* membranes that cleaves the 3-*O*-linked β-hydroxymyristoyl moiety of lipid A precursors. *J. Biol. Chem.* **274,** 11150–11158
29. Wang, X., Ribeiro, A. A., Guan, Z., McGrath, S. C., Cotter, R. J., and Raetz, C. R. (2006) Structure and biosynthesis of free lipid A molecules that replace lipopolysaccharide in *Francisella tularensis* subsp. *novicida*. *Biochemistry* **45,** 14427–14440
30. Needham, B. D., Carroll, S. M., Giles, D. K., Georgiou, G., Whiteley, M., and Trent, M. S. (2013) Modulating the innate immune response by combinatorial engineering of endotoxin. *Proc. Natl. Acad. Sci. U.S.A.* **110,** 1464–1469
31. Jennings, M. P., Srikhanta, Y. N., Moxon, E. R., Kramer, M., Poolman, J. T., Kuipers, B., and van der Ley, P. (1999) The genetic basis of the phase variation repertoire of lipopolysaccharide immunotypes in *Neisseria meningitidis*. *Microbiology* **145,** 3013–3021
32. van Kooyk, Y., Unger, W. W., Fehres, C. M., Kalay, H., and García-Vallejo, J. J. (2013) Glycan-based DC-SIGN targeting vaccines to enhance antigen cross-presentation. *Mol. Immunol.* **55,** 143–145
33. Lee, F. K., Gibson, B. W., Melaugh, W., Zaleski, A., and Apicella, M. A. (1999) Relationship between UDP-glucose 4-epimerase activity and oligoglucose glycoforms in two strains of *Neisseria meningitidis*. *Infect. Immun.* **67,** 1405–1414
34. Wakarchuk, W., Martin, A., Jennings, M. P., Moxon, E. R., and Richards, J. C. (1996) Functional relationships of the genetic locus encoding the glycosyltransferase enzymes involved in expression of the lacto-*N*-neotetraose terminal lipopolysaccharide structure in *Neisseria meningitidis*. *J. Biol. Chem.* **271,** 19166–19173
35. Moran, A. P., Prendergast, M. M., and Appelmelk, B. J. (1996) Molecular mimicry of host structures by bacterial lipopolysaccharides and its contribution to disease. *FEMS Immunol. Med. Microbiol.* **16,** 105–115
36. Puig-Kröger, A., Serrano-Gómez, D., Caparrós, E., Domínguez-Soto, A., Relloso, M., Colmenares, M., Martínez-Muñoz, L., Longo, N., Sánchez-Sánchez, N., Rincon, M., Rivas, L., Sánchez-Mateos, P., Fernández-Ruiz, E., and Corbí, A. L. (2004) Regulated expression of the pathogen receptor dendritic cell-specific intercellular adhesion molecule 3 (ICAM-3)-grabbing nonintegrin in THP-1 human leukemic cells, monocytes, and macrophages. *J. Biol. Chem.* **279,** 25680–25688
37. Jones, H. E., Copland, A., Hamstra, H. J., Cohen, J., Brown, J., Klein, N., van der Ley, P., and Dixon, G. (2013) LOS oligosaccharide modification enhances dendritic cell responses to meningococcal native outer membrane vesicles expressing a non-toxic lipid A. *Cell. Microbiol.* 10.1111/cmi.12231
38. Mata-Haro, V., Cekic, C., Martin, M., Chilton, P. M., Casella, C. R., and Mitchell, T. C. (2007) The vaccine adjuvant monophosphoryl lipid A as a TRIF-biased agonist of TLR4. *Science* **316,** 1628–1632
39. de Vries, J. J., Bungener, L., Ter Veer, W., van Alphen, L., van der Ley, P., Wilschut, J., and Huckriede, A. (2009) Incorporation of LpxL1, a detoxified lipopolysaccharide adjuvant, in influenza H5N1 virosomes increases vaccine immunogenicity. *Vaccine* **27,** 947–955
40. Steeghs, L., Keestra, A. M., van Mourik, A., Uronen-Hansson, H., van der Ley, P., Callard, R., Klein, N., and van Putten, J. P. (2008) Differential activation of human and mouse Toll-like receptor 4 by the adjuvant candidate LpxL1 of *Neisseria meningitidis*. *Infect. Immun.* **76,** 3801–3807
41. Arenas, J., van Dijken, H., Kuipers, B., Hamstra, H. J., Tommassen, J., and van der Ley, P. (2010) Coincorporation of LpxL1 and PagL mutant lipopolysaccharides into liposomes with *Neisseria meningitidis* opacity protein: influence on endotoxic and adjuvant activity. *Clin. Vaccine Immunol.* **17,** 487–495
42. Kang, T. H., Bae, H. C., Kim, S. H., Seo, S. H., Son, S. W., Choi, E. Y., Seong, S. Y., and Kim, T. W. (2009) Modification of dendritic cells with interferon-γ-inducible protein-10 gene to enhance vaccine potency. *J. Gene Med.* **11,** 889–898
43. Gupta, G., Majumdar, S., Adhikari, A., Bhattacharya, P., Mukherjee, A. K., and Majumdar, S. B. (2011) Treatment with IP-10 induces host-protective immune response by regulating the T regulatory cell functioning in *Leishmania donovani*-infected mice. *Med. Microbiol. Immunol.* **200,** 241–253
44. Xu, W., Joo, H., Clayton, S., Dullaers, M., Herve, M. C., Blankenship, D., De La Morena, M. T., Balderas, R., Picard, C., Casanova, J. L., Pascual, V., Oh, S., and Banchereau, J. (2012) Macrophages induce differentiation of plasma cells through CXCL10/IP-10. *J. Exp. Med.* **209,** 1813–1823
45. Dufour, J. H., Dziejman, M., Liu, M. T., Leung, J. H., Lane, T. E., and Luster, A. D. (2002) IFN-γ-inducible protein 10 (IP-10; CXCL10)-deficient mice reveal a role for IP-10 in effector T cell generation and trafficking. *J. Immunol.* **168,** 3195–3204